

Letters

Resilient Operation of Heterogeneous Sources in Cooperative DC Microgrids

Subham Sahoo , Member, IEEE, Tomislav Dragičević , Senior Member, IEEE, and Frede Blaabjerg , Fellow, IEEE

Abstract—As distributed control layer makes dc microgrids vulnerable toward cyber attacks, the identification and mitigation of attacked agent(s) becomes even more challenging with heterogeneity between each source based on factors, such as capacity, reliability, and generation cost. This letter proposes a novel resilient methodology, which involves detection using adaptive discord element and immediate mitigation via an event-driven approach. The proposed approach successfully mitigates cyber attacks under experimental conditions.

Index Terms—Cooperative control, cyber attacks, dc microgrid, heterogeneous sources, resilient controller.

I. INTRODUCTION

DISTRIBUTED energy management system (EMS) in dc microgrids offers a flexible and economic alternative to centralized approach [1]. It provides resiliency from single-point-of-failure, plug-and-play capability, and a reduced cost of communication infrastructure [2]. As shown in Fig. 1, the measurements from grid-forming converters (commonly termed as agents in this letter) are transmitted between each other to achieve *consensus* by accommodating average voltage regulation and power sharing, respectively. The intermittent nature of renewable energy sources, which are usually operated in grid-following mode to extract maximum power, bring asymmetry in the current sharing profiles of grid-forming converters. Moreover, different characteristics of each source and operation principle of the corresponding converters lead to the principle of heterogeneity in dc microgrids. Based on some of the prominent aspects of heterogeneity overviewed in Table I for dc microgrids [1], [3]–[4], energy management schemes often introduce an adaptive droop to be applied on local current measurements, which leads to disproportionate current sharing profile.

Manuscript received February 24, 2020; revised April 3, 2020; accepted April 25, 2020. Date of publication April 28, 2020; date of current version July 31, 2020. This work was supported by the Velux Foundations under the Villum Investigator Grant—REPEPS under Award 00016591. (Corresponding author: Subham Sahoo.)

Subham Sahoo is with the Department of Energy Technology, Aalborg University, 9220 Aalborg, Denmark (e-mail: sssa@et.aau.dk).

Tomislav Dragičević is with the Center of Electric Power and Energy, Technical University of Denmark, 2800 Kongens Lyngby, Denmark (e-mail: tomdr@elektro.dtu.dk).

Frede Blaabjerg is with the Department of Energy Technology, Aalborg University, 9220 Aalborg, Denmark (e-mail: fbl@et.aau.dk).

Color versions of one or more of the figures in this article are available online at <https://ieeexplore.ieee.org>.

Digital Object Identifier 10.1109/TPEL.2020.2991055

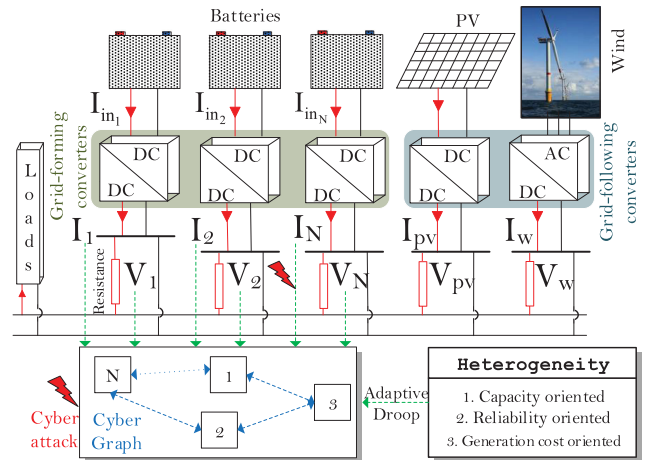


Fig. 1. Generic cyber-physical model of a dc microgrid with N grid-forming heterogeneous agents: blue and green arrows represent the cyber link and measurements/control signals, respectively; whereas, red bolts represent the attacked layers.

TABLE I
ASPECTS OF HETEROGENEITY IN DC MICROGRIDS

Heterogeneity	Design of adaptive droop ΔR_i
Capacity oriented [1]	$H_2(s)[\exp(\sum_{j \in N_i} (SoC_j(t) - SoC_i(t))) - 1]^1$
Reliability oriented [3]	$\frac{D^i}{\max_k \{D^k\}^2}$
Cost oriented [4]–[5]	$H_3(s)[\sum_{j \in N_i} (\lambda_j(t) - \lambda_i(t))]^2$

¹ $H_2(s)$ is a PI controller, SoC_j & SoC_i are the state of charge of batteries in i^{th} and j^{th} agent, N_i is the set of neighbors of i^{th} agent.

² D^i and D^k denotes the total damage and component damage (for each component k) in i^{th} converter, respectively.

³ $H_3(s)$ is a PI controller, λ_j & λ_i are the incremental costs of generation of i^{th} and j^{th} agent, respectively.

However, these measurements can be corrupted by injecting malicious data into the cyber-physical components of the microgrid [6]. Many attack detection models have been proposed to detect such attacks for proportionate current sharing [7]–[10]. However, detection of these attacks becomes more challenging with disproportionate current sharing profile. On the other hand, mitigation of these attacks is still not adequately discussed in the abovementioned papers. To the best of authors' knowledge, the only notable contribution in this area is the trust and confidence factor based resilient control in cooperative dc microgrids [11]. However, the online calculation of these factors, which

involves additional layers of integration and division operations, assigns high computational burden. Moreover to provide an attack-resilient operation, it requires a minimum of half of the neighboring converters to be *trustworthy*, thereby limiting its resilience capability for worst case attacks.

To remove the attack elements in cooperative dc microgrids, this letter proposes an adaptive discordant element (ADE) for each agent. Extending the presence of attacks as a binary mechanism using an ADE, an event-driven mitigation strategy is proposed to reconstruct and replace the attacked signal with a *trustworthy* signal. As opposed to [11], this strategy can provide resilience even using a single *trustworthy* neighboring information. The proposed resilient strategy is tested for the attacks discussed in [9] to validate its robustness in a distributed dc microgrid.

II. DESIGN OF RESILIENT CONTROL STRATEGY

In the system shown in Fig. 1 comprising N agents, each communication digraph is represented via edges to constitute an adjacency matrix $\mathbf{A} = [a_{ij}] \in R^{N \times N}$, where the communication weights are given by: $a_{ij} > 0$, if $(\psi_i, \psi_j) \in \mathbf{E}$, where \mathbf{E} is an edge connecting two nodes, with ψ_i and ψ_j being the local and neighboring nodes, respectively. Otherwise, $a_{ij} = 0$. Furthermore, the incoming cyber-information matrix can be denoted by $\mathbf{Z}_{in} = \sum_{i \in N} a_{ij}$. Hence, if \mathbf{A} and \mathbf{Z}_{in} match with each other, the Laplacian matrix \mathbf{L} is *balanced*, where $\mathbf{L} = \mathbf{Z}_{in} - \mathbf{A}$.

Using the preliminaries of the communication graph, the local control input of the cooperative secondary controller can be written as follows:

$$u_i(t) = \xi \sum_{j \in M_i} \underbrace{a_{ij}(x_j(t) - x_i(t))}_{e_i(t)} \quad (1)$$

where $u_i = \{u_i^V, u_i^I\}$, $e_i = \{e_i^V, e_i^I\}$ corresponding to the elements in $x_j = \{\bar{V}_j, R_j I_j\}$, ξ is the convergence variable, and M_i is the set of neighbors of the i th agent. Furthermore, \bar{V}_j , R_j , and I_j denote the average voltage estimate, dynamic droop, and output current of the neighboring agents, respectively. The design of dynamic droop for the i th agent is carried out using

$$R_i = R_i^o + \Delta R_i \quad (2)$$

where $R_i^o = \Delta V_i / I_i^{\max}$ is a fixed droop quantity with ΔV_i denoting an allowable voltage deviation of 5% and I_i^{\max} denoting the maximum output current for the i th converter. On the other hand, the adaptive droop for the i th agent ΔR_i can be designed based on the aspect of heterogeneity, as explained in Table I. It is worth notifying that the update for capacity- and reliability-oriented adaptive droop gains is carried out in shorter (in ms) and fairly longer (monthly) time-scale, respectively.

Using (1), the control inputs to achieve average voltage regulation and proportionate current sharing can be obtained from secondary sublayers I and II respectively by using the following voltage correction terms for the i th agent:

$$\text{Sublayer I: } \Delta V_{1_i} = H_1(s)(V_{\text{ref}} - \bar{V}_i) \quad (3)$$

$$\text{Sublayer II: } \Delta V_{2_i} = H_2(s)u_i^I \quad (4)$$

where $\bar{V}_i = V_i + \int_0^T \sum_{i \in M_i} (u_i^V d\tau)$, whereas $H_1(s)$ and $H_2(s)$ are proportional-integral (PI) controllers. Furthermore, V_{ref} is the global reference voltage quantity for all the agents. The correction terms obtained in (3) and (4) are finally added to the global reference voltage to achieve local voltage references for the i th agent using as follows:

$$V_{\text{ref}}^i = V_{\text{ref}} + \Delta V_{1_i} + \Delta V_{2_i}. \quad (5)$$

Using (5) as the local voltage reference for the i th agent, the control objectives for distributed EMSs [1], [2] in dc microgrids are achieved, which can be summarized as follows:

$$\lim_{t \rightarrow \infty} \bar{V}_i(t) = V_{\text{ref}}, \lim_{t \rightarrow \infty} u_i^I(t) = 0 \quad \forall i \in N. \quad (6)$$

However, the objectives in (6) can be misconstrued in the presence of cyber attacks on current measurements in the i th agent using

$$\text{Sensor attack: } I_i^f = I_i(t) + \kappa I_i^a \quad (7)$$

$$\text{Cyber-link attack: } I_j^f = I_j(t) + \kappa I_j^a \quad (8)$$

where $\kappa = 1$ denotes the presence of an attack element I_i^a in the i th agent, or 0 otherwise. Hence, this letter concerns the mitigation of the most sophisticated attack, namely deception attacks, where $\mathbf{I}^a = \mathbf{L}\mathbf{I}^a = 0$. Since the attack elements in deception attacks follow the cooperative synchronization theory, it leads to a feasible and stable solution. Further details about these attacks and their impact in dc microgrids with homogeneous sources can be found in [9].

To detect the presence of attack elements, we consider the average state-space voltage dynamics of each grid-forming dc/dc converter in vector form upon multiplication of \mathbf{R} on both sides given by

$$\mathbf{R}\dot{\mathbf{V}} = \mathbf{R}\mathbf{C}^{-1}(\mathbf{T}_h\mathbf{I}^{\text{in}} - \mathbf{I}^f) \quad (9)$$

where $\mathbf{T}_h = \mathbf{1} - \mathbf{T}$. Furthermore, \mathbf{I}^{in} , \mathbf{T} , \mathbf{R} , \mathbf{C} , and \mathbf{I}^f denote the diagonal matrices of the input current I_{in_i} , duty ratio T_i , dynamic droop R_i , dc link capacitance C_i , and the attacked output current measurement I_i^f , respectively, for N agents.

Considering the error in the voltage controller to be zero under steady-state conditions such that

$$\lim_{t \rightarrow \infty} \dot{V}_i(t) = V_{\text{ref}}^i. \quad (10)$$

Substituting (5) into (10) and multiplying \mathbf{L}^T on both sides, we get the steady-state solution of reference tracking as

$$\mathbf{L}^T \Delta \mathbf{V}_1 + \mathbf{L}^T \mathbf{H}_2 \mathbf{e}^{I^a} + V_{\text{ref}} \mathbf{1} = \mathbf{L}^T \mathbf{V} \quad (11)$$

where \mathbf{e}^{I^a} denotes a diagonal matrix of the error quantity e_{ij}^I in (1) including the attacked signal $I_i^f(t)$ ($\kappa = 1$), and $\Delta \mathbf{V}_1$ denotes the diagonal matrix of ΔV_{1_i} in (3) with \mathbf{H}_2 denoted as diagonal matrix of PI controller in (4). Moreover, $\mathbf{1}$ denote an identity matrix with a dimension of $N \times N$.

Remark 1: Since this letter only considers cyber attacks on current measurements, leaving the average voltage estimates uncompromised, $\mathbf{L}^T \Delta \mathbf{V}_1 = 0$ holds true [7].

Using Remark 1 to eliminate $\mathbf{L}^T \Delta \mathbf{V}_1$ in (11) and differentiating (6) w.r.t. time upon multiplication of \mathbf{R} on both sides,

TABLE II
 APPLICABILITY OF ADE UNDER DIFFERENT SCENARIOS

Scenarios	ADE_i	Remarks
Load change/line outage	$\leq \beta$	Realized in [8]-[9]
Attack under communication delay	$> \beta$	Realized in [8]-[9]
Ramp/sinusoidal attack	$> \beta$	Realized in [9]
Current sensor fault	$\leq \beta$	$FD_I^i > \rho_{FD^i}$ [8]
Converter outage under attack	$> \beta$	Realized in [8]-[9]
Line-to-line fault	-	Fault evaluation ² [9]

¹ A fault detection metric FD_I^i is proposed in [8] to differentiate between a current sensor fault and a cyber attack.

² A line-to-line fault evaluation theory is proposed in [9] to differentiate between line faults and cyber attacks.

we get

$$\mathbf{L}^T \mathbf{R} \mathbf{K}_P^{H_2} \dot{\mathbf{e}}^{Ia} + \mathbf{L}^T \mathbf{R} \mathbf{K}_I^{H_2} \mathbf{e}^{Ia} - \mathbf{L}^T \mathbf{R} \dot{\mathbf{V}} = 0. \quad (12)$$

As already explained in [9], $\mathbf{L}^T \mathbf{e}^{Ia} = 0$ and $\mathbf{L}^T \mathbf{C}^{-1} \mathbf{I}^f = 0$ will hold true for deception attacks. Using these equalities after substituting (9) into (12), we obtain

$$\mathbf{L}^T \mathbf{R} \mathbf{K}_P^{H_2} \dot{\mathbf{e}}^{Ia} - \mathbf{L}^T \mathbf{R} \mathbf{C}^{-1} \mathbf{T}_h \mathbf{I}^{in} = 0. \quad (13)$$

Remark II: Due to the injected attack signal, the first term of (13) will be asymmetric, not obeying the consensus theory. For (13) to hold true, this property will be reflected in the second term of (13), which becomes the basis of detection for deception attacks in cooperative dc microgrids with heterogeneous sources.

Since the proposed detection concept for heterogeneous sources (operating with an adaptive droop ΔR_i) is basically inspired from [8] and [9], it is termed as ADE in this letter, which can be mathematically represented for the i th agent using Remark II as

$$ADE_i = l_i \left[\sum_{j \in M_i} a_{ij} (R_j I_j^{in} - R_i I_i^{in}) \right] \left[\sum_{j \in M_i} a_{ij} (R_j I_j^{in} + R_i I_i^{in}) \right]. \quad (14)$$

It is worth notifying that the proposed detection criteria is scalable to N agents, which has been largely discussed in [8] and [9]. Since ADE exceeds β only in the presence of cyber attacks on current measurements, it guarantees robust and accurate detection performance under many scenarios including sensor and line-to-line faults, which has been detailed in Table II. Some of the scenarios in Table II have been simulated for ADE in Fig. 2, where ADE_2 goes beyond $\beta (=0.02)$ only for cyber attacks on agent II irrespective of their nature. On the other hand, ADE_2 stays within the detection band β for load change and sensor faults. In fact, sensor faults are detected via a fault detection metric FD_I^2 exceeding $\rho_{FD^i} (=0.02)$ [8], thereby differentiating sensor faults with deception attack.

Even though a discord element based detection strategy was proposed in [9], a timely mitigation technique to remove these attacks was still not discussed. As the robustness of the proposed attack detection strategy is guaranteed using Table II, this letter uses an event-driven signal reconstruction based mitigation strategy based on a follow-up signal from ADE_i to provide resilience

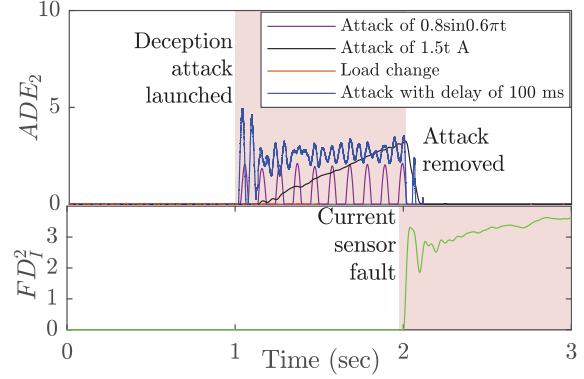


Fig. 2. Performance of ADE for various cyber attacks at $t = [1, 2]$ s and the fault detection metric FD_I [8] for current sensor fault at $t = [2, 3]$ s.

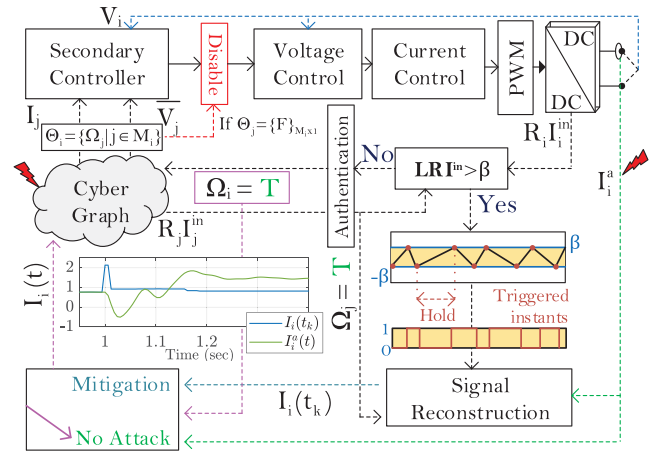


Fig. 3. Proposed resilient strategy in the i th agent to mitigate deception attacks in a dc microgrid with heterogeneous sources—red bolts depict cyber attack.

against such attacks. Upon detection of the presence of attack element in the i th agent using (14), an authentication label Ω_i is generated for the current measurements in the i th agent to alarm the presence of attack element in its neighbors. It should be noted that the nature of authentication label is binary such that

$$\Omega_i = \begin{cases} 0(\text{F}), & \text{if } ADE_i > \beta \\ 1(\text{T}), & \text{else} \end{cases} \quad (15)$$

where β is a small value detection threshold to disregard measurement noise yet ensure accurate detection. To simplify the representation of authentication for any signal, 0^T and 0^F will be used to symbolize True and False for the communicated measurements, respectively, using (15).

As long as (15) holds true, the control variables used in designing ADE_i are forced to follow the trajectories of non-compromised neighboring signals (with Ω_j labeled as True). As highlighted in Fig. 3, if the set of authentication signals Θ_i for the i th agent is not a zero vector in the presence of attack elements, event-driven resilient signals are reconstructed to mitigate deception attacks in system with heterogeneous sources

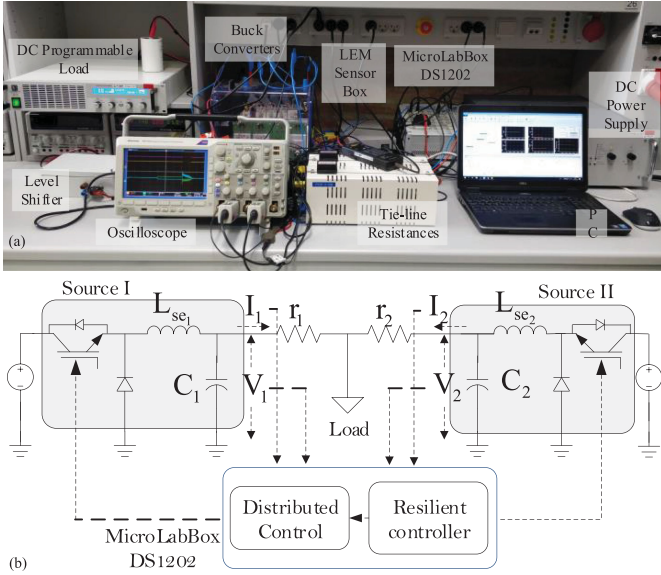


Fig. 4. (a) Experimental setup of a cooperative dc microgrid comprising $N = 2$ agents controlled by dSPACE MicroLabBox DS1202 supplying power to a programmable load. (b) Single-line diagram of the experimental setup.

using

$$I_i(t_k) = \Xi_1 \left[\frac{R_j I_j^T(t)}{R_i} \right] \quad (16)$$

where $\circ(t_k)$, with k as the triggering instant, denote the event-triggered samples of the output current in the i th agent. It is worth notifying that $\Xi[\circ]$ in (16) is a triggering function, which holds the input signal \circ until the next instant of triggering. These event-driven signals are generated when the triggering criterion ($\mathbf{LRI}^{\text{in}} > \beta$) in Fig. 3 is activated in the attacked agent. However, if Θ_i is a null vector, this implies that all the remaining agents are compromised with attack elements and should be prevented from being used in the i th agent. Hence, this leads to localized operation of the i th agent (as shown in Fig. 3).

The resilient action is completed by substituting the event-driven resilient signals with the attacked signal based on the local authentication signal using

$$I_i(t) = \Omega_i I_i^f(t) + (1 - \Omega_i) I_i(t_k). \quad (17)$$

Finally, the signal obtained in (17) is substituted into (1) to realize the mitigation of deception attacks in dc microgrids. As soon as the reconstructed signal in (17) obeys (6), the authentication label transmitted to the neighbors is switched back to T. The proposed strategy not only mitigates the attacks, but allows to operate normally under external disturbances, such as load change and communication delay.

III. EXPERIMENTAL RESULTS

The proposed detection strategy has been experimentally validated in a dc microgrid operating at a voltage reference V_{ref} of 64 V with $N = 2$ heterogeneous sources, as shown in Fig. 4(a). The entire physical layer along with flow of control signals is detailed in Fig. 4(b). Both the sources have been made to regulate the average voltage and share load current to regard the reliability

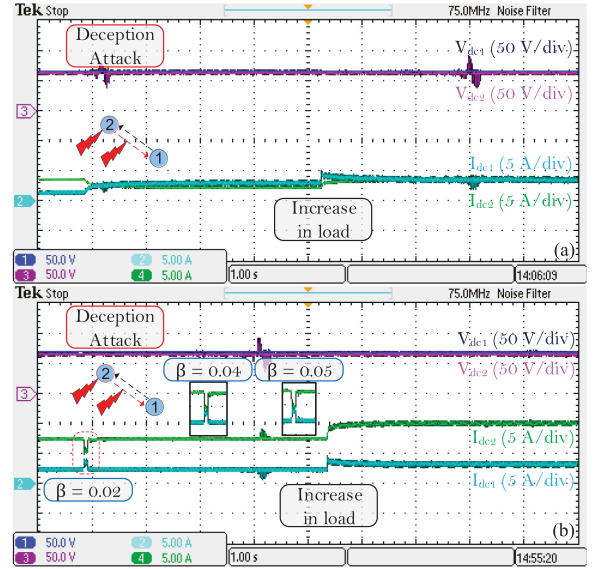


Fig. 5. Performance of a dc microgrid [shown in Fig. 4(b)] for a deception attack on agent II (a) in the absence and (b) in the presence of the proposed resilient strategy.

of converters for enhancing the lifetime of components. Using the local and neighboring measurements, the proposed resilient strategy shown in Fig. 3 is modeled for every converter to mitigate the attacks and meet the control objectives in (6). The experimental testbed parameters along with the adaptive droop gains are provided in appendix.

In Fig. 5(a), before the deception attack is launched on agent II, agent II shares the load current in higher proportion as compared to agent I. This sharing proportion can be explained by severe ageing of component(s) in source I. When the attack is launched on agent II, it can be seen that the currents are being shared almost equally in the absence of the proposed resilient controller. As a result, reliability-oriented sharing between dc sources is clearly disregarded due to the attack. However, in the presence of the proposed resilient controller, ADE_2 is immediately activated when the deception attack is launched and adjusts the authentication label of signals from agent II to F. As per the proposed resilience mechanism, I_1^T is immediately transmitted to reconstruct $I_2(t)$ as per (16). This action allows the system to return back to the normal operating condition (preattack loading level). Additionally, it can be seen in Fig. 5(b) that the dynamic performance varies for different values of the threshold β . Intuitively, the settling time increases as the value of β increases from 0.02 to 0.05. This adjudges β to be as small as possible for faster settling time, yet it has to be sufficiently larger than the measurement noise to avoid unnecessary triggering. Moreover, it can be clearly justified that the resilient mechanism performs satisfactorily for steady-state conditions as well as disturbances, such as load change. The action is so fast that it easily accommodates an increase in load immediately following the deception attack.

Finally, in Fig. 6(a), when a worst case deception attack is launched on both agents, the current sharing proportion between the converters is reversed in the absence of resilient controller, which disregards the aspect of reliability of components in

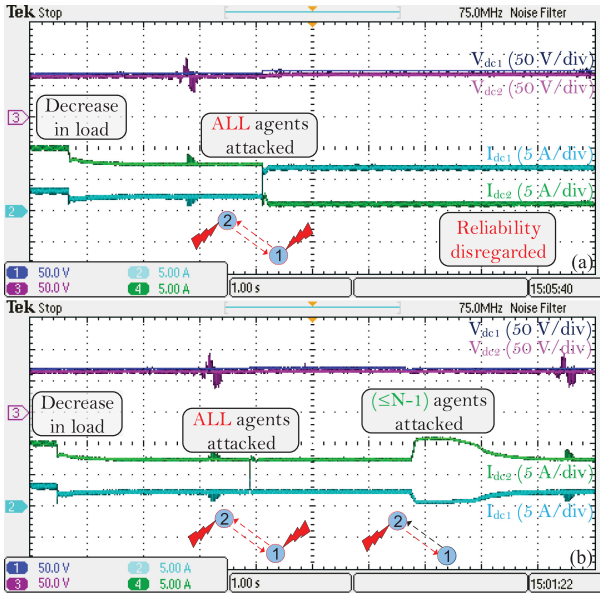


Fig. 6. Performance of dc microgrid [shown in Fig. 4(b)] for deception attacks on agents I and II simultaneously (a) in the absence and (b) in the presence of the proposed resilient strategy.

power electronic converters. This issue has been addressed by the proposed resilient controller in Fig. 6(b) where the sharing proportion between the converters is retained as per the preattack loading levels to regard reliability. Since the authentication pool Θ_i is F for both agents, the signal reconstruction algorithm holds the preattack instant throughout the period. It is worth notifying that any load change under these circumstances will lead to local operation (disabled secondary controller, as shown in Fig. 3). Nevertheless when the attack element is removed from agent I, it can be seen that the system returns back to the normal operating condition following a transient using the authenticated $I^{T_1}(t)$. Hence, this validates the effectiveness of the performance of the proposed resilient controller to a maximum of $(N - 1)$ scale attacks (at least one *trusted* agent will always be required in the system to broadcast *True* signals). This establishes that the proposed resilient mechanism can be easily scaled to many applications in dc-based power electronic systems.

IV. CONCLUSION

A novel resilient control strategy is proposed to mitigate the most sophisticated form of cyber attacks in dc microgrids. As opposed to the existing work, this strategy is simple and can

be readily applied to any distributed EMSs for dc microgrids comprising heterogeneous sources. Additionally, this strategy can be easily scaled up to any number of units since only one *trusted* agent is required to reconstruct *trustworthy* signals, thereby removing the attack. This theory has been validated experimentally to show the robustness and ease of implementation for mission-critical applications, such as naval ships and electric aircrafts, where reliability and security are of prime concern.

APPENDIX

EXPERIMENTAL PARAMETERS

The considered system consists of two sources with the converters rated equally for 600 W. It should be noted that the controller gains are consistent for each converter.

Plant: $L_{se_i} = 3$ mH, $C_i = 100$ μ F, $r_1 = 0.8$ Ω , and $r_2 = 1.4$ Ω .

Controller: $V_{ref} = 64$ V, $K_P^{H_1} = 1.92$, $K_I^{H_1} = 15$, $K_P^{H_2} = 4.5$, $K_I^{H_2} = 0.08$, $l = 1.36$, $\xi = 1.8$, $\beta = 0.02$, $R^o = 0.5$, $\Delta R_1 = 0.05$, and $\Delta R_2 = 0.4$.

REFERENCES

- [1] S. Sahoo, S. Mishra, S. Jha, and B. Singh, "A cooperative adaptive droop based energy management and optimal voltage regulation scheme for DC microgrids," *IEEE Trans. Ind. Electron.*, vol. 67, no. 4, pp. 2894-2904, Apr. 2020.
- [2] S. Sahoo and S. Mishra, "A distributed finite-time secondary average voltage regulation and current sharing controller for DC microgrids," *IEEE Trans. on Smart Grid*, vol. 10, no. 1, pp. 282-292, Jan. 2019.
- [3] S. Peyghami, P. Davari, and F. Blaabjerg, "System-level reliability-oriented power sharing strategy for DC power systems," *IEEE Trans. Ind. Appl.*, vol. 55, no. 5, pp. 4865-4875, Sep./Oct. 2019.
- [4] Z. Lv, *et al.*, "Distributed economic dispatch scheme for droop-based autonomous DC microgrid," *Energies*, vol. 13, no. 2, 2020, Art. no. 404.
- [5] S. Sahoo and J. C. -H. Peng, "A localized event driven resilient mechanism for cooperative microgrid against data integrity attacks," *IEEE Trans. Cybern.*, to be published, doi: [10.1109/TCYB.2020.2989225](https://doi.org/10.1109/TCYB.2020.2989225).
- [6] S. Sahoo, T. Dragicevic, and F. Blaabjerg, "Cyber security in control of grid-tied power electronic converters—Challenges and vulnerabilities," *IEEE J. Emerg. Sel. Topics Power Electron.*, to be published.
- [7] S. Sahoo, S. Mishra, J. C.-H. Peng, and T. Dragicevic, "A stealth cyber-attack detection strategy for DC microgrids," *IEEE Trans. Power Electron.*, vol. 34, no. 8, pp. 8162-8174, Aug. 2019.
- [8] S. Sahoo, J. C.-H. Peng, S. Mishra, and T. Dragicevic, "Distributed screening of hijacking attacks in DC microgrids," *IEEE Trans. Power Electron.*, vol. 35, no. 7, pp. 7574-7582, Jul. 2019.
- [9] S. Sahoo, J. C.-H. Peng, A. Devakumar, S. Mishra, and T. Dragicevic, "On detection of false data in cooperative DC microgrids—A discordant element approach," *IEEE Trans. Ind. Electron.*, vol. 67, no. 8, pp. 6562-6571, Aug. 2020.
- [10] O. Beg, L. V. Nguyen, T. T. Johnson, and A. Davoudi, "Signal temporal logic-based attack detection in DC microgrids," *IEEE Trans. Smart Grid*, vol. 10, no. 4, pp. 3585-3595, Jul. 2019.
- [11] S. Abhinav, H. Modares, F. L. Lewis and A. Davoudi, "Resilient cooperative control of DC microgrids," *IEEE Trans. Smart Grids*, vol. 10, no. 1, pp. 1083-1085, Jan. 2019.